Temporal-Variance Weighted P-space Multipole Frequency Mapping

Kyle S Decker[1,2] and Chunlei Liu[3,4]

[1]*Center for In Vivo Microscopy, Duke University, Durham, NC, United States,* [2]*Biomedical Engineering, Duke University, Durham, NC, United States,* [3]*Brain Imaging and Analysis Center, Duke University, Durham, NC, United States,* [4]*Radiology, Duke University, Durham, NC, United States*

PURPOSE: The recently developed **p**-space method allows susceptibility tensor imaging (STI) without any rotation of the subject or magnetic field [1,2]. The **p**-space is sampled using pulsed field gradients or shifted image reconstruction and provides anisotropic multipole frequency variation within a voxel [2]. We have previously shown that there is a non-linear temporal signal evolution of white matter (WM) in the **p**-space [3]. The dependence of the higher-order multipole frequency on echo time (TE) can be used to weight the **p**-space multipole frequency maps, resulting in enhanced WM anisotropy and contrast. The resulting temporal-variance weighted multipole frequency maps provide a new contrast mechanism sensitive to susceptibility effects.

METHODS: Applying a single shifted image reconstruction for a given **p**-vector allows us to generate orientation-specific multipole frequency maps in the **p**-space. An appropriate **p**-value (shift) was chosen to optimize contrast between gray matter (GM) and WM regions. Ex-vivo imaging was performed on adult 10-week old C57BL/6 mice that were anesthetized and perfusion fixed. Images were acquired on a 9.4 T (400 MHz) 89-mm vertical bore Oxford magnet controlled by a GE EXCITE MR imaging console. The scanner used a shielded coil providing gradients of 2200 mT/m. A 3D spoiled-gradient-recalled-echo (SPGR) sequence was used with the following parameters: matrix size = 512x256x256, field-of-view (FOV) = 22x11x11 mm^3, bandwidth (BW) = 62.5 kHz, flip angle = 60°, TR = 100 ms. The scan was repeated for a TE of 4.4, 7, 9, 11, 13, and 15 ms.

Laplacian based phase unwrapping and background field removal, HARPERELLA [4], was performed for the phase images at each TE. The processed phase images were combined with the corresponding magnitude images in order to form the phase-corrected complex data. Similarly, for each shift in the **p**-space a complex average of the shift in the positive and negative direction was performed. **p**-space multipole frequency maps (f_{TE}) were reconstructed for the three orthogonal orientations: [1 0 0], [0 1 0], and [0 0 1] using a **p**-value of 0.48, 0.48, and 0.46 respectively at each TE. A weighted average of multipole frequency maps (f_{ME}) based on SNR was computed for TEs with sufficient frequency SNR (echoes 1-4). Similarly, the multipole frequency variance across these echoes (δf) was computed for each **p**-space orientation, and the resulting variance was median filtered using a kernel of 3x3x3 voxels (δf_{filt}). The filtered variance was then used to weight the average **p**-space multipole frequency map in a multiplicative manner ($\delta f_{ME} * \delta f_{filt}$). Fig. 1 depicts the process for orientation [1 0 0] by showing all the intermediate steps and final result.

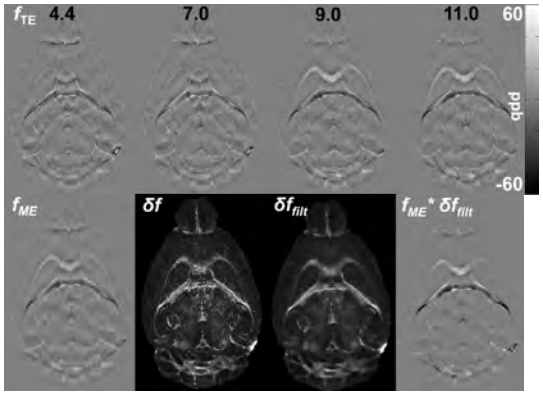

Fig. 1. Overview of temporal-variance weighted **p**-space multipole frequency mapping. Top row shows p-space frequency maps at each TE (f_{TE}). Bottom row shows f_{ME}, resulting from weighted average of first 4 TEs, δf which is the variance across the same TEs, δf_{filt}, the filtered variance, and $\delta f_{ME} * \delta f_{filt}$, the average frequency multiplied by filtered variance.

RESULTS: Implementing HARPERELLA on the phase data prior to any **p**-space analysis and performing a complex average of the shift in the positive and negative direction for each **p**-value significantly reduced artifacts in the **p**-space multipole frequency maps resulting from a single **p**-value, thus suppressing false variations across echoes. Fig. 2a shows the resulting multipole frequency map for TE = 9 ms with neither of the two processing steps implemented. Artifacts are clearly visible as highlighted by red arrows in the image. Fig. 2b shows the multipole frequency map resulting from averaging the positive and negative shift. The severe artifacts are reduced but some irregularities are still apparent. Fig. 2c shows the multipole frequency map resulting from both previously mentioned processing steps. There are no significant artifacts present. The temporal-variance weighted **p**-space multipole frequency maps for the three orthogonal orientations are shown in Fig. 3. There is excellent WM/GM contrast in each representative orientation, and clear anisotropy which can be visualized by looking at the difference image between orientations [1 0 0] and [0 1 0]. The multipole frequency of GM is significantly suppressed in all orientations, allowing an isolated characterization of the WM anisotropy.

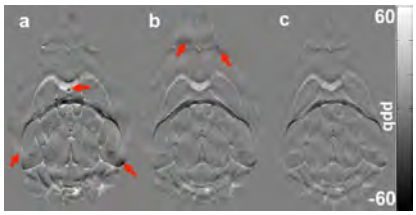

Fig. 2. Original **p**-space multipole frequency maps with no processing (a), average of +/- shifts (b), and unwrapped and filtered phase data with averaging of +/- shifts (c). Artifacts are highlighted by red arrows.

DISCUSSIONS AND CONCLUSIONS: Higher-order multipole frequency distribution in the **p**-space is characterized by a non-linear dependence on TE in WM regions, whereas GM regions show little to no dependence on TE [3]. As a result, the temporal-variance is dominant in the WM, leading to enhanced WM and suppressed GM regions respectively in the **p**-space multipole frequency maps when using the temporal variance as a weighting factor. Orientation dependence of zeroth-order phase in MRI arises from the presence of ordered bundles of axons in the WM. These axons are surrounded by myelin sheath, believed to possess radial susceptibility anisotropy [5]. Our proposed temporal-variance weighted **p**-space multipole frequency mapping allows clear visualization of higher-order frequency anisotropy, thus allowing the analysis of sub-voxel anisotropy.

This method could be readily applied in-vivo to characterize and better visualize neurological diseases affecting the WM, such as multiple sclerosis (MS). The demyelinated WM lesions could be easily identified because they have reduced or diminished anisotropy. Similarly, the temporal-variance determined in this method can be analyzed to determine how TE dependence changes in different anatomical regions of the WM.

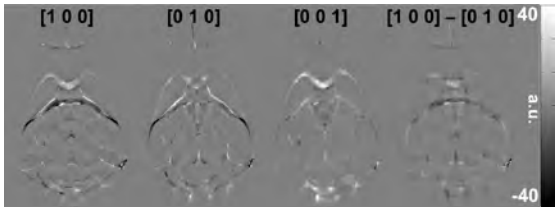

Fig. 3. Temporal-variance weighted **p**-space multipole frequency maps corresponding to the three orthogonal orientations. The difference map between orientations [1 0 0] and [0 1 0] shows clear WM anisotropy.

REFERENCES: 1. Liu, C., MRM 2010; 63:1471-1477. 2. Liu, C. and Li, W. NeuroImage 2013; 67:193-202. 3. Decker, K. and Liu, C. Proc of 3rd QSM Workshop 2014: 95. 4. Li, W. et al. NMR Biomed 2014; 27:219-227. 5. Wharton, S. and Bowtell, R. PNAS 2012 ; 109:18559-19564.